Single-Quantum Annihilation of Positrons

HIROMASA MAZAKI, MASATSUGU NISHI, AND SAKAE SHIMIZU
Institute for Chemical Research, Kyoto University, Kyoto, Japan

(Received 19 February 1968)

Total cross sections for the single-quantum annihilation of positrons in five elements have been measured. The monoenergetic positron beam was obtained by the use of a Siegbahn-Slätis intermediate-image spectrometer mounted with a Na^{22} source. Thin foils of $_{50}Sn$, $_{73}Ta$, $_{79}Au$, $_{82}Pb$, and $_{92}U$ were used, successively, as targets mounted at the focal point of the spectrometer. The monoenergetic γ photons due to the single-quantum annihilation was measured in coincidence with accompanying K x rays from the target, using the NaI(Tl) scintillation detectors. The effect of the finite target thickness was evaluated carefully by measuring the energy distribution of incident positrons in the thin target. The exponent of Z in the total cross section of this process for the incident positrons with 300-keV kinetic energy has been found to be 4.93 ± 0.31, in agreement with calculations by Johnson *et al.* The energy dependence of the total cross sections, measured for $_{82}Pb$ and $_{92}U$ in the positron energy range from 250 to 400 keV, has also been found to be in fairly good agreement with theoretical values calculated by other workers using the relativistic Coulomb wave functions for both the K-shell electron and the incident positron.

I. INTRODUCTION

ALTHOUGH there are several modes to be considered in the process of positron annihilation, the most probable of these is, as is well known, the two-quantum annihilation of positrons almost at rest. In the nuclear field, however, positrons in flight have a probability of annihilating with atomic bound electrons (mostly K-shell electrons) and giving rise to the single-quantum annihilation (SQA). The first theoretical prediction of this mode of annihilation was proposed by Fermi and Uhlenbeck[1] in 1933. In the following years, some other theoretical works[2–5] were also reported. More recently, the total cross section of SQA has been calculated by Johnson *et al.*[6] for several high-Z elements using relativistic Coulomb wave functions for both the K-shell electron and the incident positron. Their results showed pretty good agreement with those previously reported by Jaeger and Hulme.[5]

The experimental study of this phenomenon was first carried out by Meric[7] in 1950, but because of the poor experimental techniques available in those days, only rough qualitative conclusions could be achieved. In the last few years, more refined measurements of the total cross section of SQA have been performed by Sodickson *et al.*[8] and Flammersfeld *et al.*[9,10] Both results show good agreement as to the energy dependence, and both support the calculations with relativistic Coulomb wave functions; but with respect to the Z dependence, their measurements lead to quite different conclusions.

In the process of SQA, neglecting the very small recoil energy of the nucleus concerned, the energy of the emitted photon, E_γ, can be given by the following simple relation:

$$E_\gamma = 2m_0c^2 + E_p - B_K, \quad (1)$$

where m_0 is the electron rest mass, E_p is the kinetic energy of the positron, and B_K is the binding energy of the K-shell electron in the target atom. Since E_p is the kinetic energy of the positron in the instant of undergoing SQA, in the experimental practice E_p should be $E_0 - \Delta E$, where E_0 denotes the initial kinetic energy of a positron falling upon the target material and ΔE is the positron energy loss in the target before it gives rise to SQA.

In principle, there are two ways of observing SQA of positrons. One is measurements with a thick target, in which all incident positrons may annihilate in flight or at rest by emitting one, two, or more quanta. In this thick-target experiment, the observed spectrum of SQA photons is supposed to show a continuous energy distribution ranging between the extreme values $E_{\gamma\,\max} = 2m_0c^2 + E_0 - B_K$ and $E_{\gamma\,\min} = 2m_0c^2 - B_K$. Furthermore, in this case, the ratio of background radiation due to the two-quantum annihilation to the number of SQA photons becomes quite large, because the total cross section of the two-quantum annihilation increases rapidly over that of SQA when the positron energy decreases. The other way of measuring SQA is with a thin target, where only a part of the incident positrons can annihilate in flight and most of them pass through the target without annihilating. In contrast to the former method, in the thin-target experiment ΔE can be expected to be so small that in Eq. (1), E_p can be considered to be nearly equal to E_0, and thus the emitted SQA hard γ's would be monoenergetic. Owing to the

[1] E. Fermi and G. E. Uhlenbeck, Phys. Rev. **44**, 510 (1933).
[2] H. J. Bhabha and H. R. Hulme, Proc. Roy. Soc. (London) **A146**, 723 (1934).
[3] Y. Nishina, S. Tomonaga, and H. Tamaki, Sci. Pap. Inst. Phys. Chem. Res. (Tokyo) **24**, Suppl. No. 18, 7 (1934); **27**, 178 (1935).
[4] H. A. Bethe, Proc. Roy. Soc. (London) **A150**, 129 (1935).
[5] J. C. Jaeger and H. R. Hulme, Proc. Cambridge Phil. Soc. **32**, 158 (1936).
[6] W. R. Johnson, D. J. Buss, and C. O. Carroll, Phys. Rev. **135**, A1232 (1964).
[7] S. Meric, Rev. Fac. Sci. Univ. Istanbul **15A**, 136 (1950); **15A**, 179 (1950).
[8] L. Sodickson, W. Bowman, J. Stephenson, and R. Weinstein, Phys. Rev. **124**, 1851 (1961).
[9] H. Langhoff, H. Weigmann, and A. Flammersfeld, Nucl. Phys. **41**, 575 (1963).
[10] H. Weigmann, H. Hansen, and A. Flammersfeld, Nucl. Phys. **45**, 555 (1963).

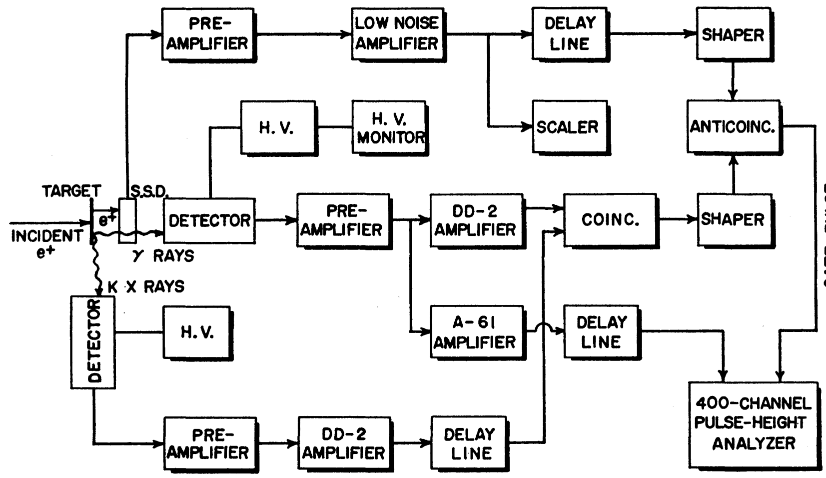

FIG. 1. Block diagram of the electronic circuitry.

reason mentioned above, the thin-target experiment should be more favorable, in spite of the smaller counting rate of SQA photons.

In the present paper, we report details of our experimental work performed with the intention of providing additional information on the Z and energy dependence of the total cross section σ by means of the thin-target experiment. Since the total cross section of SQA is predicted to peak at around 300 keV of positron kinetic energy,[5,6] our interest was focused on the comparatively low-energy range. The Z dependence of σ was studied with five targets of different Z's, i.e., $Z=50$, 73, 79, 82, and 92 for the 300-keV positrons, while the energy dependence was observed only for the last two elements in the energy range of 250–400 keV. In the present work careful procedures have been pursued for evaluation of the detection efficiency of the measuring system and the effect of the finite target thickness.

II. APPARATUS

Using a β-ray spectrometer, positrons with kinetic energies between 250 and 400 keV were focused on thin-disk targets of five different elements. Since the counting rate of the SQA photons was supposed to be very low because of the small cross section of the phenomenon to be observed, the main effort of the present experiment was made to eliminate the background radiation. Whenever a positron annihilates in a target by emitting one photon, it is accompanied by the K x ray (or, with less probability, the outer-shell characteristic x ray) of the atom concerned. This fact easily led us to a possible way of reducing the large background by applying the coincidence technique for the SQA photons and accompanied K x rays. Moreover, in order to eliminate the false and chance coincidences involved, we also used an anticoincidence circuit connected to a surface-barrier silicon detector. This detector placed just behind the target foil was adopted for detection of the positrons that passed through the target without giving rise to the annihilation. The positron signals from the silicon detector were fed, with those of coincidences, into the anticoincidence circuit and the output signals were used as the gate pulses for a TMC 400-channel pulse-height analyzer. The block diagram of the measuring electronic circuitry is shown in Fig. 1.

Since the cross section of the SQA process is rather small, the thicknesses of the target foils of pure elements had to be chosen by reflecting on some favorable experimental conditions. The thickness of each target was chosen so as to be approximately one-fifth of the range of focused positrons,[11] taking account of their energy and angle of incidence onto the target being 60°. The thicknesses of the target foils of 8 mm in diameter used in the present experiment are listed in Table I. In the following sections are described some details of the β-ray spectrometer, the detectors, and the other apparatus used.

TABLE I. Ranges of 300-keV positrons in the targets of different atomic number Z and target thicknesses used in the present work.

Target	Positron range[a] (mg/cm²)	Target thickness (mg/cm²)
$_{50}$Sn	144	31.2
$_{73}$Ta	159	33.2
$_{79}$Au	163	31.6
$_{82}$Pb	166	31.5
$_{92}$U	174	29.5

[a] Data are taken from the table prepared by Nelms (Ref. 11).

A. β-Ray Spectrometer

A Siegbahn-Slätis intermediate-image spectrometer mounted with a Na^{22} source of about 3 mCi was used to obtain the monoenergetic positron beam incident upon a target. Since we preferred the number of positrons incident upon a target to be as large as possible, the annular slit situated at the midpoint of the spectrometer

[11] A. T. Nelms, Natl. Bur. Std. (U.S.) Circ. No. 577 (1956).

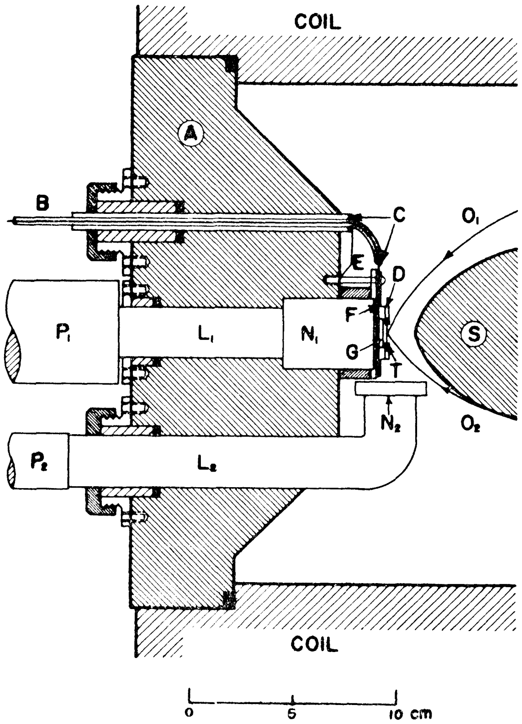

FIG. 2. Experimental arrangement of the target and detectors in the β-ray spectrometer: (A) pole piece of the spectrometer; (B) shielded lead to supply bias voltage to the surface-barrier silicon detector; (C) Araldite vacuum seal; (D) target holder; (E) earthing line; (F) Teflon plate as an insulator; (G) surface-barrier silicon detector for detection of positrons passed through the target; (T) target; (N_1 and N_2) NaI(Tl) crystals for the SQA photons and K x rays, respectively; (L_1 and L_2) Lucite light-guide pipes; (P_1 and P_2) Toshiba 7696 and EMI 9524S photomultipliers, respectively; (O_1 and O_2) positron trajectories, distance from the axis and vertical projection, respectively; (S) central lead γ-ray stop.

and the other slit set in front of the Na^{22} source were opened unusually, and consequently the momentum resolution of the spectrometer became rather poor. Making use of a surface-barrier silicon detector with a window of 8 mm in diameter placed at the focus of the spectrometer, we measured the relation of transmission and resolution of the spectrometer for the internal K-conversion line of the 662-keV transition from a point source of Cs^{137}. From the measurements it was indicated that for the present purpose the momentum resolution was not critically deteriorated up to a 2.5-mm annular slit width and an 18-mm opening of the source-side slit. For the maximum permissible slit widths given above, the momentum resolution of this spectrometer was found to be about 8.0% for the focus limited to 8 mm in diameter.

At the focus-side pole piece of the spectrometer, as shown in Fig. 2, are mounted the thin-foil target and three different detectors, the surface-barrier silicon detector covered with the foil target to be irradiated by the monoenergetic positron beam, a NaI(Tl) crystal for the SQA photons with a Lucite light-guide pipe, and a thin NaI(Tl) crystal for the K x rays with a curved Lucite light-guide pipe.

B. Detectors

The main detector is a 30-mm-diam and 40-mm-thick NaI(Tl) scintillator used for measurements of the SQA photons. In order to catch most of the SQA photons emitted from the target this crystal is mounted only 6 mm from the target. A Lucite light-guide pipe, 2.4 cm in diameter and 7.8 cm long, is axially mounted between the crystal and photomultiplier. Of particular importance in the present measurement is the stability of the photomultiplier for the γ-ray detector. To obtain maximum stability, careful examinations of several kinds of phototubes were carried out and a Toshiba 7696 phototube, of which long-term instability was proved to be less than $\pm 0.5\%$ per week under normal experimental conditions, was finally employed. Evaluation of the detection efficiencies ϵ_γ of this γ-ray detector for the SQA photons is rather complicated. Details of this procedure are described in Sec. III.

As the x-ray detector, a thinner NaI(Tl) crystal of 25-mm diam and 4-mm thickness was used. As shown in Fig. 2, this detector was placed perpendicular to the target and connected to an EMI 9524S photomultiplier through a curved Lucite light-guide pipe. The x-ray detection efficiencies ϵ_x for the K x rays from different Z targets were evaluated using the 32-keV x ray from Cs^{137}, the 88-keV γ ray from Cd^{109}, and the 122-keV γ ray from Co^{57}. Circular pieces of filter paper 8 mm in diameter, wetted by the solutions of these radioactive nuclides, were used as the sources, of which absolute intensities were determined otherwise by the usual method employing a scintillation detector. The source thus prepared was placed just at the place for the target foil and the x- or γ-ray spectrum was observed *in situ* by the x-ray scintillation detector. From these measurements we could evaluate the necessary values of ϵ_x as follows:

$$\epsilon_x = 3.76\times10^{-2} \quad \text{for} \quad K \text{ x rays from } {}_{50}\text{Sn (25.8 keV)},$$

$$\epsilon_x = 3.15\times10^{-2} \quad \text{for} \quad K \text{ x rays from } {}_{73}\text{Ta (58.9 keV)},$$

$$\epsilon_x = 2.93\times10^{-2} \quad \text{for} \quad K \text{ x rays from } {}_{79}\text{Au (70.5 keV)},$$

$$\epsilon_x = 2.83\times10^{-2} \quad \text{for} \quad K \text{ x rays from } {}_{82}\text{Pb (76.7 keV)},$$

$$\epsilon_x = 2.37\times10^{-2} \quad \text{for} \quad K \text{ x rays from } {}_{92}\text{U (100.8 keV)}.$$

The errors in these values are estimated to be $\pm 5\%$, almost independent of Z.

A surface-barrier silicon detector with the depletion depth of about 280 μ for 100 V detector bias was employed to count the number of positrons passed through the target. The thickness of a gold layer of the detector surface was 5 $\mu g/cm^2$ and the energy resolution of this detector was estimated to be about 3.5% for 300-keV positrons. Since the detection efficiency including the backscattering effect of positrons from the surface was not known for this specific detector, its counting rate was compared to that of a Geiger-Mueller (G-M) counter with an 8-mm-diam window made of a rubber hydrochloride film of 0.625-mg/cm^2 thickness. Taking into consideration the resolving time of this G-M counter, the annular slit of the spectrometer was covered by a brass baffle with only 1% open area to reduce the number of incident positrons. Supposing that the detection efficiency of this G-M counter be 100%, that of the silicon detector was estimated to be 95±5% for the 300-keV positrons. With this silicon detector, monitoring of the number of positrons impinging on the target per unit time was often made in the course of the present experiment.

III. DETECTION EFFICIENCY OF THE γ-RAY DETECTOR

In order to determine the total cross section of SQA, the detection efficiency of the γ-ray scintillation detector for the SQA photons concerned should be evaluated for the actual experimental arrangement. Since the geometrical arrangement of the detectors and target foil is not simple, we have to take into consideration the following factors: angular distribution of the SQA photons emitted from the target, obstructing effect of the surface-barrier silicon detector mounted between the target and the γ-ray detector, and backscattering of γ rays produced by the annihilation processes in the target from the surroundings in the spectrometer.

We calculated first the theoretical photopeak efficiencies of the γ-ray detector for the energies of SQA photons which were assumed to be emitted from a circular plane source of 8 mm in diameter placed on the crystal axis and 6 mm from its surface. Johnson[12] has recently shown theoretically that the SQA photons have a sharp angular distribution in the forward direction of incident positrons. In our calculations we took account of the angular distribution of the emitted SQA photons in accordance with this prediction. On the basis of some reasonable assumptions, the calculations were carried out by the Monte Carlo method with an aid of Kyoto University's KDC-II computer.[13] The assumptions adopted are as follows: (a) The monoenergetic positron beam incident upon the 8-mm-diam disk target at an angle of 60° to the crystal axis is uniformly distributed over the surface of target. (b) The angular distribution of incident positrons in the target is taken into account, but their energy loss is neglected. Consequently, it is assumed that the resulting SQA photons be monoenergetic. (c) Only three processes are taken into consideration as primary events for γ rays in the NaI crystal, i.e., the Compton scattering, photoelectric effect, and pair production, while the coherent scattering is neglected. (d) All secondary electrons and positrons scattered or created by the primary processes would be stopped in the crystal and all their kinetic energy absorbed by the crystal. (e) The x rays due to the photoelectric effect would be absorbed completely in the crystal. (f) The secondary γ rays traced are those due to Compton scattering and two 511-keV annihilation γ's emitted in the opposite direction to each other immediately after the creation of positrons.

With this simplified model of processes, the history of an incident γ ray was simulated; the number of histories traced was 10 000. In the present case the cross sections for these interactions of γ rays in NaI were taken from the table prepared by Grodstein.[14] The calculated photopeak efficiencies thus obtained, ϵ_t, could not, however, be used directly for our purpose, because, as described above, our geometrical arrangement of the detector and target system was rather complicated and the obstructing effect of the surface-barrier silicon detector as well as the backscattering of the γ rays concerned should be taken into consideration. For this reason, as the next step, the calculated photopeak efficiencies have to be corrected by taking the experimental conditions into account.

Three disk sources of Cs^{137}, Zn^{65}, and Na^{22} of 8 mm in diameter were prepared by wetting pieces of filter paper with solutions containing each of these γ-ray-emitting nuclides. Their absolute intensities were determined by means of photofractions calculated by Miller *et al.*[15] Then, we observed the pulse-height spectra of these sources using the γ-ray detector with the light-guide pipe, where the measurements were performed *in situ*, i.e., the source was mounted at just the same place as the target foil, and the geometry of the detectors and others in the spectrometer was maintained quite similar to that used for the measurements of the SQA photons. Combining the observed photopeaks of the spectra of 662-keV (Cs^{137}), 1115-keV (Zn^{65}), and 1277-keV (Na^{22}) γ rays and the absolute intensities of these sources, respectively, we could estimate the photopeak efficiencies of the present γ-ray detector for these γ rays. From these data the photopeak efficiencies could be estimated for the photons which would be expected for the SQA process to be studied. It is, however, noted that the values thus obtained, denoted as ϵ_i, are useful only for the photons emitted isotropically from the circular plane sources *in situ*.

On the other hand, we calculated the theoretical photopeak efficiencies of the NaI(Tl) crystal for γ rays with the energies in question emitted isotropically from

[12] W. R. Johnson, Phys. Rev. **159**, 61 (1967).

[13] Kyoto University digital computer No. 2; commercial name is HITAC-5020.

[14] Gladys White Grodstein, Natl. Bur. Std. (U.S.) Circ. No. 583 (1957).

[15] W. F. Miller, J. Reynolds, and W. J. Snow, Argonne National Laboratory Report No. ANL-5902, 1958 (unpublished).

TABLE II. Detection photopeak efficiencies of the γ-ray detector, ϵ_γ, for the SQA photons with energy E_γ.

Target	Positron energy (keV)	E_γ (keV)	ϵ_γ [a]
$_{50}$Sn	300	1275	8.84×10^{-3}
$_{73}$Ta	300	1238	8.70×10^{-3}
$_{79}$Au	300	1224	7.87×10^{-3}
$_{82}$Pb	250	1172	9.04×10^{-3}
$_{82}$Pb	300	1220	7.97×10^{-3}
$_{82}$Pb	400	1327	7.44×10^{-3}
$_{92}$U	250	1145	8.85×10^{-3}
$_{92}$U	300	1193	7.96×10^{-3}
$_{92}$U	400	1300	6.80×10^{-3}

[a] Errors in these values are estimated to be $\pm8\%$, almost independent of E_γ.

the 8-mm-diam circular plane source placed on the axis of the crystal and 6 mm from its surface. The calculations were performed also by the Monte Carlo method, based upon the same reasonable assumptions as those adopted in the case of ϵ_t mentioned above. The calculated values are denoted by ϵ_t'.

Combining the numerical values ϵ_t, ϵ_i, and ϵ_t' obtained by the theoretical and experimental procedures mentioned above, for the practical photopeak efficiencies of the γ-ray NaI(Tl) detector applicable for our purpose we adopted $\epsilon_\gamma=\epsilon_t(\epsilon_i/\epsilon_t')$. This way of estimating ϵ_γ is believed to be a close approximation without an appreciable error. The numerical values of ϵ_γ evaluated by this procedure and used in the present work are listed in Table II. The errors in these values are estimated to be $\pm8\%$, mainly caused by uncertainty in measurements of photopeaks in the spectra using the prepared sources and in measurements of their absolute intensities.

IV. EXPERIMENTAL PROCEDURE

A. Source Preparation

The Na^{22} source was prepared from radioactive sodium chloride solution (3 mCi, 0.5*N*) of high specific activity obtained from Nuclear Science & Engineering Corp. The solid contained in the solution used was expected to be less than 0.4 mg. Since the most intolerable trouble that may take place in the process of source preparation is erosion of a backing metal by the acid solution, a preliminary examination of source preparation was made using a 0.5*N* HCl solution so as to keep the solid production minimum. A tantalum disk having a well-type hole (2.4 mm in diameter and 0.9 mm in depth) was finally chosen as the backing and the evaporation residuum of the radioactive solution of Na^{22} was mounted in the hole. Using this source we could obtain 8.5×10^5 positrons per minute at the focus of the β-ray spectrometer when the momentum was selected to be 300 keV.

B. Measurements of γ-Ray Spectra

After eliminating most of the background radiation by applying the coincidence ($2\tau=60$ nsec) and anticoincidence ($2\tau=45$ nsec) techniques, the spectra of γ rays generated in the targets were accumulated using a 400-channel pulse-height analyzer. The γ-ray signals were discriminated at a level corresponding to about 400 keV, whereas the window for the x-ray signals was fully opened, because in the latter case it was not possible to distinguish the x-ray signals from those of noise owing to the distortion of the spectrum. The energy calibration of the analyzer was repeated at appropriate intervals using γ rays from Na^{22} and Zn^{65}, while the whole performance of the measuring system was also checked at least two times a day using standard pulses from a pulse generator.

The measurements of γ spectra were carried out for about 200 h for each target to be studied in order to ensure the statistical reliability of the data. Furthermore, the energy dependence of the cross section in the range of 250–400 keV of incident positron energies was investigated similarly for lead and uranium. In Figs. 3 and 4 are shown the observed spectra after subtracting stray γ-ray and natural backgrounds.

According to Johnson's work[12] on the angular distribution of SQA photons, most of them produced in a thin target are emitted in the forward direction of the incident positrons. To confirm his prediction, we modified our geometrical arrangement, i.e., the γ-ray detector was moved 20 mm back (to the left-hand side in Fig. 2) from the original position (6 mm from the target). Comparison of the spectra observed at the different positions of the detector for the lead target is of particular interest because in the modified geometry most of the SQA photons are supposed not to be

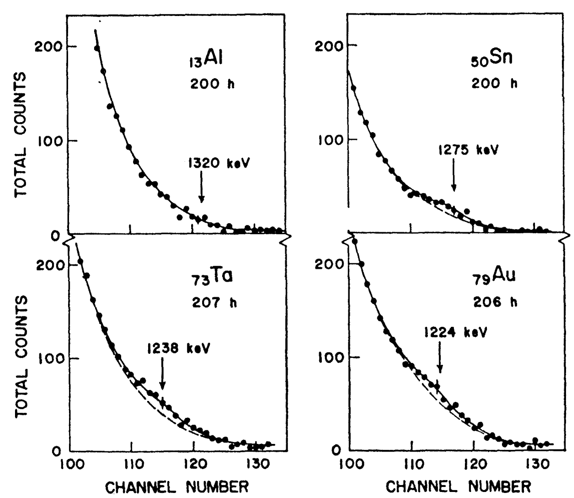

FIG. 3. Observed SQA peaks for the 300-keV incident positrons. In the case of the aluminum target, no evidence of the peak due to the SQA photons is observed.

counted by the detector. Careful study of these two spectra demonstrated that the SQA photons could be observed by the original geometry employed in the present work but not by the modified geometry indicating the sharp angular distribution of the SQA photons as well as their existence itself.

C. Evaluation of Effect of Finite Target Thickness

For estimation of the total cross section of SQA, the effective number of positrons which may contribute to the SQA process in the target should be reasonably evaluated. For this purpose, we must take into consideration the loss of incident positrons in the target of finite thickness. The total loss of positrons in the target can be easily obtained by measuring the difference of positron numbers with and without a target. However, this information is not sufficient to know the actual positron flux in the target, because in such a thin target the flux can not be expected to show a simple exponential decrease, but has somewhat complicated shape. For this reason we have attempted to find the positron flux in the targets used in the present work by observing the energy spectra of positrons passed through the thinner targets of various thicknesses. From the data thus obtained, the number of positrons being able to contribute to SQA and also the most probable energy loss of incident positrons in the targets, $\langle \Delta E \rangle$, can be determined.

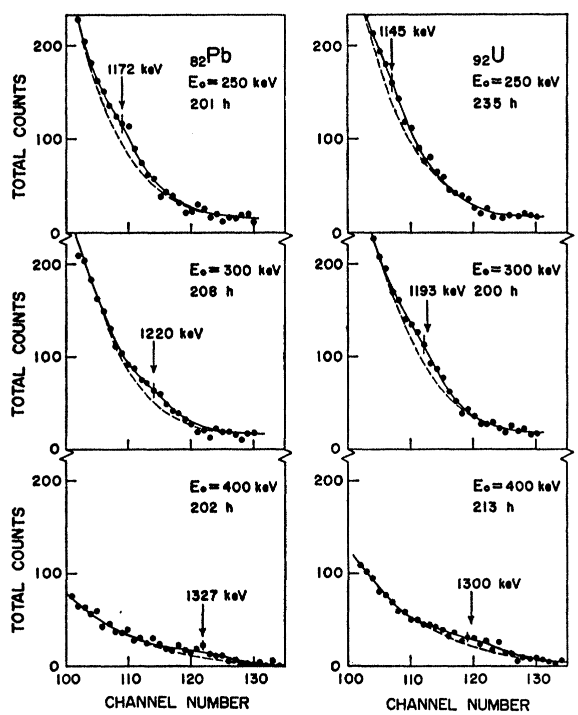

FIG. 4. Observed SQA peaks for the 250-, 300-, and 400-keV incident positrons onto the lead and uranium targets.

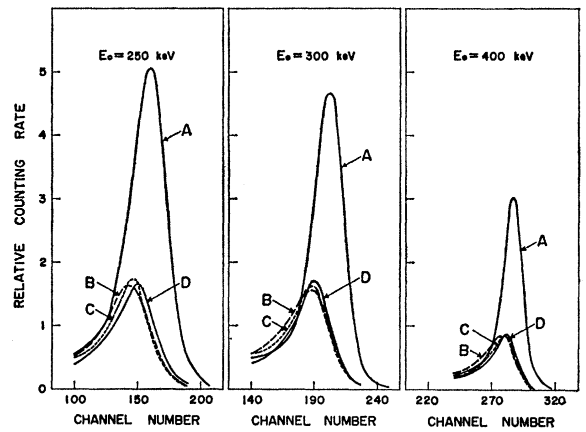

FIG. 5. Energy distributions of positrons in the target used: (A) incident positrons; (B) energy distribution in the tin target (31.2 mg/cm^2); (C) in the gold target (31.6 mg/cm^2); and (D) in the lead target (31.5 mg/cm^2).

Using tin, gold, and lead foils, we first prepared several thin targets with different thicknesses, i.e., tin, 4.2, 7.0, 14.0, 22.0, 28.0, and 31.2 mg/cm^2; gold, 8.9, 16.8, 24.6, and 31.6 mg/cm^2; and lead, 7.9, 15.4, 25.8, and 31.5 mg/cm^2. The thickest target of each element is that used in the measurements of SQA. Then, each of these targets attached on a Li-drifted silicon detector was mounted at the focus of the β-ray spectrometer and the energy spectra of the positrons incident upon the target with the selected momentum of 250, 300, and 400 keV were measured by this silicon detector of 2.0% energy resolution. Each positron spectrum observed with the thinner target is considered to give the energy spectrum of positrons inside the thickest target of the corresponding element, neglecting the backscattering effect of positrons in the target.

Taking a channel number of the pulse-height analyzer as a parameter, and plotting the number of positrons accumulated in the channel as a function of thickness, the distributions of positrons with certain kinetic energies throughout the thickest targets are obtained. By summing up the total number of positrons falling in each channel and plotting it again as a function of energy, we can get the energy spectra of the positrons in the tin, gold, and lead targets used for the measurements of SQA. In Fig. 5 are shown the resulting energy spectra obtained after these procedures mentioned above.

Comparison of these spectra with the one observed without a target gives a fraction of the incident positrons that may contribute to the SQA peak to be observed for each target, denoted as C_p, and also the most probable energy loss of incident positrons in the target, $\langle \Delta E \rangle$. By applying the usual interpolation and extrapolation method, those for the tantalum and uranium targets were also determined after proper corrections for the target thicknesses. The numerical results thus

TABLE III. Fraction of incident positrons that may contribute to SQA, C_p, and the most probable energy loss of incident positrons in the target, $\langle \Delta E \rangle$.

Target[a]	Positron energy (keV)	C_p	$\langle \Delta E \rangle$ (keV)
$_{50}$Sn	300	0.483±0.029	18±2
$_{73}$Ta	300	0.455±0.027	17±2
$_{79}$Au	300	0.442±0.027	17±2
$_{82}$Pb	250	0.328±0.020	12±2
$_{82}$Pb	300	0.412±0.025	14±2
$_{82}$Pb	400	0.492±0.030	7±2
$_{92}$U	250	0.320±0.019	11±2
$_{92}$U	300	0.390±0.023	13±2
$_{92}$U	400	0.488±0.029	6±2

[a] Target thicknesses are given in Table I.

obtained are listed in Table III. As is described in Sec. V, C_p was used as a correction factor for the effect of the finite target thickness when we estimated the total cross section of SQA. $\langle \Delta E \rangle$ was used for the evaluation of the energy of emitted SQA photons via Eq. (1).

D. Measurement of Backgrounds

The most predominant source of the backgrounds involved in the γ-ray spectrum arises from the two-quantum annihilation of positrons in the target. The maximum energy of the photons created by this annihilation in flight is about 980 keV for the 300-keV positrons incident on a lead target. This energy is much lower than that of the SQA photons; nevertheless for the poor resolution of the measuring system, there seems to be still some contribution from this mode of annihilation at the higher-energy region. The probability of the two-quantum annihilation is, as has been well established, a function of NZ, where N is the number of target atoms per unit area with Z electrons per atom. From this viewpoint, the spectrum of annihilation γ rays was observed with an aluminum target of 25.9-mg/cm^2 thickness, being nearly equivalent to that of the lead target with respect to the two-quantum annihilation. However, fitting of two spectra of γ rays from the two-quantum annihilation process in aluminum and lead targets was not absolutely satisfactory even after proper normalization. This slight discrepancy may be caused by the fact that there are some other factors involved in these spectra, such as the scattered γ rays. This notwithstanding, it should be pointed out that at the expected position of the spectrum with the aluminum target no evidence of the existence of SQA photons was observed (see Fig. 3), for which one can plausibly give the explanation from the strong Z dependence of the cross section.

The contribution of 1277-keV γ rays from Na^{22}, if any, may give rise to serious errors in the estimations of the cross section. In order to check this, a careful 200-h measurement was carried out after closing the annular slit of the spectrometer so as to stop all positrons and to observe only the strayed γ-ray and natural backgrounds. Fortunately, it was proved that the background due to the 1277-keV γ rays did not contribute critically to the SQA peak. Thus we were justified in concluding that the observed small peaks at about 1.2 MeV are certainly due to the SQA photons.

V. RESULTS AND DISCUSSION

As shown in Figs. 3 and 4, the peaks due to the SQA photons are observed as to grow more remarkably with increasing Z of the target elements. However, there is scarcely any peak due to this process in the spectrum obtained with the aluminum target. Since our γ-ray detector was attached with the long Lucite light-guide pipe, its energy resolution was found to be rather poor. The long tail in the high-energy region of the observed spectrum with the aluminum target can be explained by attributing it to the γ rays from the two-quantum annihilation in flight. The dashed lines under the peaks showing the background are drawn as the most reasonable ones taking into account the spectrum obtained with the aluminum target. The energy values given above the peaks in the figures show the energies of the SQA photons expected from Eq. (1). As already discussed in Sec. IV C, the positrons contributing to the SQA process have an energy distribution in the target concerned and subsequently the probability of SQA is not exactly same for each positron with different kinetic energy. Nevertheless, because energy loss of positrons in the target is rather small and the predicted total cross section of SQA is nearly constant in the energy region in question, we introduced the most probable energy loss $\langle \Delta E \rangle$ given in Table III, for the evaluation of E_γ.

In order to determine the most reasonable profiles of the SQA peaks, the observed curves of energy distribution of positrons in the target and the energy resolution of the γ-ray detector should be taken into account. The profile of the observed SQA peak can be expressed by

$$F(E_\gamma) = \int_0^{E_p\,\max} P(E_p) \exp\{-(E_\gamma - E_p - 2m_0c^2 + B_K)^2/2\delta^2\}\, dE_p, \tag{2}$$

where $P(E_p)$ is the energy distribution of positrons in the target. The function $P(E_p)$ can be obtained by the observations shown in Fig. 5. The quantity δ in this equation is the standard deviation of the observed photopeak, the shape of which is assumed to be a Gaussian distribution, and can be given by $\Gamma = 2.355\delta$, where Γ is the photopeak full width at half-maximum (FWHM) observed by the γ-ray detector for the monoenergetic photons in the energy region in question. The photopeak FWHM was measured *in situ* using the 1277-keV γ rays from Na^{22} and a value of about 160 keV found was adopted as Γ. The function $F(E_\gamma)$ was obtained by numerical calculations of Eq. (2) for each observed SQA peak. After pursuing this complicated procedure we could draw the most reasonable profiles of the SQA peaks as shown in Figs. 3 and 4.

From the SQA peak thus obtained we have attempted to evaluate the total cross section for SQA. The cross section σ can be given by the following expression:

$$\sigma = N_\gamma / N_p N \epsilon_\gamma \epsilon_x C_a C_p. \qquad (3)$$

The symbols in the expression are as follows:

N_γ = the number of the observed SQA photons per unit time,

N_p = the number of positrons incident upon the target per unit time,

N = the effective number of atoms in the target per unit area,

ϵ_γ = the detection efficiency of the γ-ray detector for the SQA photons,

ϵ_x = the detection efficiency of the x-ray detector,

C_a = the correction factor for the loss of true coincidences by chance anticoincidences,

C_p = the correction factor for the effect of the finite target thickness for the incident positrons.

N_γ was estimated from the peak appearing at the expected position of the observed γ-ray spectrum shown in Figs. 3 and 4. N_p was measured at times by using the surface-barrier silicon detector placed at the focus of the β-ray spectrometer. N can be easily obtained from the known surface density of the target concerned. ϵ_γ was estimated by the procedure described in Sec. III and its values used in the present work are listed in Table II, while ϵ_x was determined experimentally by the method described in Sec. II B. For the use of the anticoincidence circuit connected with the coincidence (see Fig. 1), there may be some loss of the true coincidence signals by chance. The correction factor C_a, introduced in Eq. (3) for this possible loss of the true signals of the SQA photons, can be given by

$$C_a = (N_1 - 2\tau N_1 N_2)/N_1, \qquad (4)$$

where τ denotes the resolving time of the anticoincidence circuit, N_1 is the number of the true coincidences, and N_2 is the number of positrons passed through the target and detected by the silicon detector. As the maximum evaluation, the value of C_a was found to be 0.998, which is quite negligible. The correction factor C_p is of particular importance, because it would be a source of serious error in the final result. Therefore, as described in Sec. IV C, we performed careful measurements of C_p, numerical values of which are listed in Table III.

By inserting numerical values of these factors into the right-hand side of Eq. (3), we obtained the values of the total cross sections, which are given in Figs. 6 and 7, as a function of atomic number Z and of positron kinetic energy, respectively. The errors shown are estimated from those for the factors in Eq. (3). The main

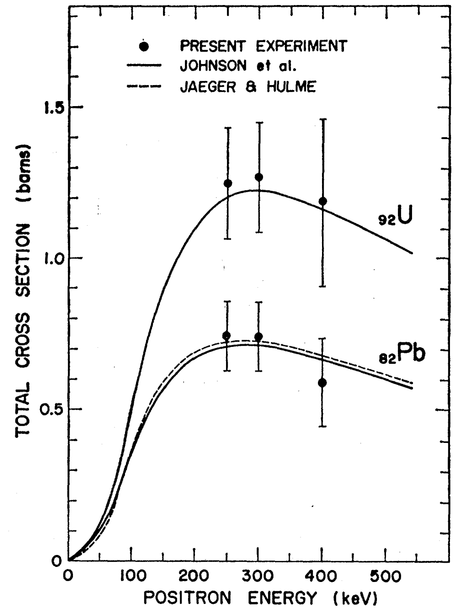

FIG. 7. Energy dependence of the total cross sections of SQA for the lead and uranium targets. The kinetic energies of incident positrons are 250, 300, and 400 keV. Solid curves are the theoretical results calculated by Johnson *et al.* (Ref. 6) and dashed curve is by Jaeger and Hulme (Ref. 5).

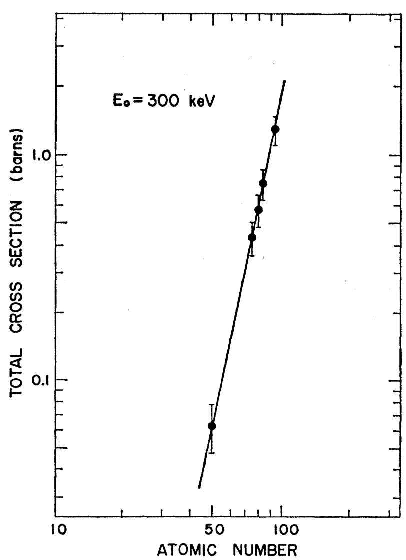

FIG. 6. The total cross sections of SQA for the targets of different atomic number Z, i.e., $Z=50$, 73, 79, 82, and 92. The kinetic energy of incident positrons is 300 keV.

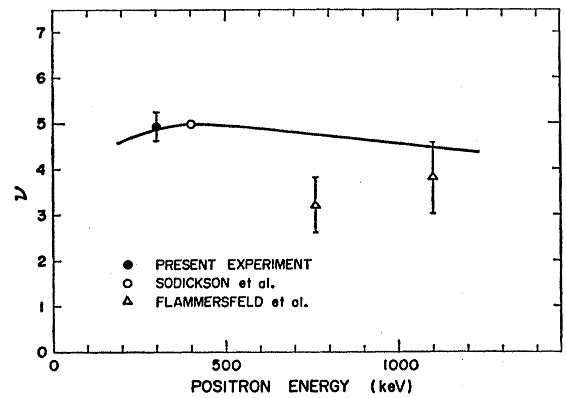

FIG. 8. Exponent of atomic number Z in the total cross section of SQA, ν, versus kinetic energy of incident positrons. Solid circle is the result of the present work for $E_0=300$ keV. Open circle is the experimental result given by Sodickson *et al.* for $E_0=400$ keV (Ref. 8) and triangles are the results reported by Flammersfeld *et al.* for $E_0=760$ and 1100 keV (Ref. 10). The theoretical value of ν calculated by Johnson *et al.* (Ref. 6) is also shown by a solid curve for comparison.

uncertainty involved in the final result is due to that in the estimation of N_γ from the observed spectra, in spite of cautious procedures pursued for the background estimation and shaping of the most reasonable profile of the SQA peak as described before. Because of the poor resolution of the present γ-ray detector, the possible, but small contribution from SQA by the L-shell electrons may be involved in the observed SQA peaks. However, in the present experiment this contribution to N_γ is neglected for the reason that the probability of causing SQA with different shell electrons is proportional to n^{-3} (n is the principal quantum number), and thus the drawing of a reasonable profile of the SQA peak due to the L-shell electrons can not be achieved statistically. Our final results, therefore, can be accepted as those concerned with SQA by only the K-shell electrons in the target atoms.

The exponent of Z in the total cross section ν was found from the result shown in Fig. 6, by applying a least-squares analysis, to be 4.93 ± 0.31 for the positrons with kinetic energy $E_p=300\text{ keV}-\langle\Delta E\rangle$. It is noted that since the values of $\langle\Delta E\rangle$ are rather small compared with the incident energy of 300 keV as described in Sec. IV C, the total cross sections measured can be accepted as those for the positrons with kinetic energy of 300 keV within the experimental error. The values of ν revealed experimentally by the present and previous works[8,10] are shown in Fig. 8 in comparison with the theoretical result deduced from calculations by Johnson *et al.*[6] In the figure, for these experimental values the kinetic energies of the incident positrons onto the targets are taken as those of positrons undergoing SQA with K-shell electrons. The result obtained by the present work for the 300-keV incident positrons shows good agreement with the theoretical value calculated using relativistic Coulomb wave functions for both the K-shell electron and the incident positron. The values of ν for 760 and 1100 keV measured by Flammersfeld *et al.*[10] are smaller than the theoretical prediction. The SQA rates measured by Sodickson *et al.*[8] with $_{73}$Ta, $_{74}$W, $_{78}$Pt, $_{79}$Au, $_{82}$Pb, and $_{90}$Th for the 400-keV incident positrons are scattered considerably around the assumed line for $\nu=5$ in the figure of log(SQA rate) versus log$Z$ (see Fig. 6 of Ref. 8); nevertheless they concluded the Z dependence of the total cross section to be Z^5, which is shown by only an open circle without error bar in Fig. 8. As shown in Fig. 7, the energy dependence of the total cross sections obtained for lead and uranium is in fairly good agreement with the theoretical calculations by Johnson *et al.*[6] and Jaeger and Hulme[5] within the experimental error.

Reflecting on our work reported here, how to evaluate the effect of the finite target thickness is one of the key points of the experiment. If it were possible to use a stronger source of positrons and a detection system with better energy resolution for the SQA photons and x rays, thinner targets could be used to minimize this effect with an expectation of obtaining more refined results. It is also hoped that the measurement of the angular distribution of SQA photons for comparison with the theoretical result recently published by Johnson[12] will be performed.

ACKNOWLEDGMENTS

The authors are indebted to the late S. Shimodaira for his cooperation in the primary stage of the experiment. We are also grateful to Dr. W. R. Johnson for communicating to us his work prior to publication, and to Dr. S. Barkan, *née* Meric, for valuable discussions.